Research Article

Title:

Formation of intracellular vesicles within the Gram$^+$ *Lactococcus lactis* induced by the overexpression of caveolin-1β

Authors: Flourieusse A[1], Bourgeois P[1], Schenckbecher E[1], Palvair J[1], Legrand D[1], Labbé C[1], Bescond T[1], Avoscan L[2], Orlowski S[3], Rouleau A[1], Frelet-Barrand A[1].

Affiliations

1 FEMTO-ST Institute, UMR 6174, CNRS, Université Bourgogne Franche-Comté, 15B Avenue des Montboucons, CEDEX, 25030 Besançon, France

2 Agroecology Agro Dijon Institute, CNRS, INRAE, Burgundy University, Bourgogne Franche-Comté University, DImaCell, Dijon, France

3 CEA/Institut Joliot/SB2SM, CNRS/I2BC (UMR9198), Université Paris-Saclay, Gif-sur-Yvette, France

Corresponding author: annie.frelet-barrand@femto-st.fr

Abstract

Background: Caveolae are invaginated plasma membrane domains of 50-100 nm in diameter involved in many important physiological functions in eukaryotic cells. They are composed of different proteins, including the membrane-embedded caveolins and the peripheric cavins. Caveolin-1 has already been expressed in various expression systems (*E. coli,* insect cells,

Toxoplasma gondii, cell-free system), generating intracellular caveolin-enriched vesicles in *E. coli*, insect cells and *T. gondii*. These systems helped to understand the protein insertion within the membrane and its oligomerization. There is still need for fundamental insights into the formation of specific domains on membrane, the deformation of a biological membrane driven by caveolin-1, the organization of a caveolar coat, and the requirement of specific lipids and proteins during the process. The aim of this study was to test whether the heterologously expressed caveolin-1β was able to induce the formation of intracellular vesicles within a Gram$^+$ bacterium, *Lactococcus lactis*, since it displays a specific lipid composition different from *E. coli* and appears to emerge as a good alternative to *E. coli* for efficient overexpression of various membrane proteins.

Results: Recombinant bacteria transformed with the plasmid pNZ-HTC coding for the canine isoform of caveolin-1β were shown to produce caveolin-1β, in its functional oligomeric form, at a high expression level unexpected for an eukaryotic membrane protein. Electron microscopy revealed several intracellular vesicles from 30 to 60 nm, a size comparable to *E. coli* h-caveolae, beneath the plasma membrane of the overexpressing bacteria, showing that caveolin-1β is sufficient to induce membrane vesiculation. Immunolabelling studies showed antibodies on such neo-formed intracellular vesicles, but none on plasma membrane. Density gradient fractionation allowed the correlation between detection of oligomers on Western blot and appearance of vesicles measurable by DLS, showing the requirement of caveolin-1β oligomerization for vesicle formation.

Conclusion: *L. lactis* cells can heterologously overexpress caveolin-1β, generating caveolin-1β enriched intracellular neo-formed vesicles. These vesicles might be useful for potential co-

expression of membrane proteins of pharmaceutical interest for their simplified functional characterization.

Keywords

Lactococcus lactis, membrane proteins, caveolin-1, intracellular vesicles

Introduction

Caveolae are flask-shaped invagination of the plasma membrane of mammalian cells of 50 to 100 nm of diameter [1]. Involved in many physiological functions (mechanosensing, signalling, endocytosis, lipid homeostasis), they are highly abundant in muscle cells, adipocytes, endothelial cells and fibroblasts, and linked to many diseases including cardiovascular diseases, cancers, degenerative muscular dystrophies and kidney diseases [2-6]. Caveolae are essentially linked to the presence in the plasma membrane of the caveolin proteins, mainly caveolin-1 and -3 [7], and cavins (cavin1-4) [8]. Deletion of either caveolin-1 or cavin-1 leads to the loss of caveolae. Both N- and C-termini of caveolin-1 (21-24 kDa) have been shown to reside within the cytoplasm, the N-terminus segment harboring the oligomerization domain [9] while the intramembrane domain, with its helix-break-helix motif, is believed to contribute to the formation of a curved membrane thanks to a wedge effect [10]. The protein undergoes multiple modifications during membrane trafficking from synthesis site to plasma membrane [8], including oligomerization which appeared shortly after biosynthesis and association with lipids [11-12]. Caveolin oligomerization and formation of membrane domains enriched in cholesterol, phosphatidylserine and glycosphingolipids, in the

presence of cavins, are believed to be critical for caveolae formation in mammalian cells [1,13-15].

Caveolin-1, isoforms α and β, have already been expressed in various heterologous expression systems. These systems helped to provide relative high amounts of protein, which are necessary to perform structural and functional studies, to understand the way the protein is inserted within the membrane and how it undergoes oligomerization. Moreover, it is also essential to provide fundamental insights into the formation of specific domains on membrane, the deformation of a biological membrane driven by caveolin-1, the organization of a caveolar coat, and the requirement of specific lipids and proteins during the process. Caveolin-1, isoforms α and β, have been expressed in *E. coli* [16-17], insect cells [18-20], *Toxoplasma gondii* [21], and cell-free system [22]. In all these systems (except cell-free), the expression of the recombinant caveolin induced the formation of intracellular vesicles within the heterologous host. Notably, in these few expression systems, both whole and truncated versions of caveolin-1 have been demonstrated to be sufficient alone to promote membrane budding and protrusion, and the eventual formation of intracellular vesicles presenting high homogeneity of size and shape, provided local concentration of the protein is high enough [23]. Such intracellular vesicles, called “heterologous caveolae” [17], could be used for diverse biotechnological purposes, and especially for co-expression of other membrane proteins (MPs) of interest [20,24].

The various expression systems available for heterologous expression of MPs are either prokaryotic, such as the most common *E. coli*, or eukaryotic (yeasts, insect cells, mammalian cells). They display different features in terms of lipid composition and cellular machinery, with respective advantages and drawbacks while expressing MPs. Among them,

the bacterial expression system *Lactococcus lactis* has emerged since 2000 as a good alternative to *E. coli* for expression of MPs, in particular for eukaryotic MPs [25-29]. Indeed, in contrast to *E. coli*, it displays interesting features for expression and further studies of MPs: it does not form inclusion bodies [26] and has only one membrane, that presents a specific lipid composition. Moreover, a tightly controlled system (NICE, NIsin-Controlled gene Expression [30]), based on the use of sub-inhibitory amounts of the antimicrobial compound nisin, has already been successfully used for functional expression and characterization of MPs from diverse origins (plants, bacteria, and mammals) and functional families (ABC transporters, mitochondrial carriers and others; for review, see [29]).

Here, we describe the heterologous expression of caveolin-1β in *L. lactis*, using the NICE system, and analyze whether the protein was able to induce the formation of intracellular vesicles within this Gram$^+$ bacterium.

Material and methods

Bacterial strains and growth conditions

The strains used in this study are listed in Table 1. Lactococcal strains were grown on M17 medium (BK012HA, Biokar Diagnostics) supplemented either with 0.5% glucose (M17G medium) at 30°C without shaking for DNA isolation or with 1% glucose (M17G1) at 30°C with gentle shaking (90 rpm) for induction of expression. *E. coli* strains were grown in Luria-Bertani (LB) medium (L3522, Merck) at 37°C with shaking (180 rpm). Antibiotics were used for plasmid maintenance at the following final concentrations: chloramphenicol (10 µg/mL) for *L. lactis* and kanamycine (100 µg/mL) for *E. coli*.

Table 1: Bacterial strains and plasmids used in this study

			Relevant genotype or phenotype	References or sources
Strains	*E. coli*			
		DH5α	F- ϕ80lacZΔM15 Δ(lacZYA-argF)U169 recA1 endA1 hsdR17(rk-, mk+) phoA supE44 thi-1 gyrA96 relA1 λ-	Invitrogen
	L. lactis			
		NZ9000	MG1363 pepN::nisRK	Ozyme
		NZ9700	Progeny of the conjugation between nisin producer strain NIZO B8 with MG1614 (RifR StrpR derivative of MG1363). Nisin producer strain for induction experiments	NIZO
Plasmids				
	pKL-HTC	plasmid containing the caveolin gene	Kanr	collaborators
	pNZ8148		Chlr	Ozyme
Kanr and Chlr: resistance to kanamycine and chloramphenicol, respectively				

Cloning for caveolin-1β expression in pNZ8148

The gene of canine caveolin-1β (Cav1β, Uniprot P33724.2, 32-178) cloned into the pKL vector [20] with a 10-His affinity tag and TEV protease site at the N-terminus of the gene (HTC for His-tag-TEV-caveolin) was used for subcloning into pNZ8148. First, a mutation was performed to insert the restriction site *Nco*I at the start codon using the QuickChange Lightning Site-Directed Mutagenesis kit (Agilent) following the manufacturer's instructions with the primer pKL-NcoIm fwd and rev (Table 2). The kanamycin-resistant clones obtained

were tested by digestion with *Nco*I and *Nde*I (NEB, Ipswich, USA) after extraction using the Nucleospin Plasmid kit (Macherey-Nagel) and following the manufacturer's instructions. The corresponding cDNA was excised from mutated pKL/HTC by digestion with *Nco*I and *Sac*I (NEB, Ipswich, USA) following the manufacturer's instructions and ligated into pNZ8148NS previously digested with the same endonucleases. The two ligation reactions were purified, eluted, and then used to transform NZ9000 strain by electroporation [31]. Chloramphenicol-resistant clones were selected on M17GChl Agar Petri dishes after 1–2 days at 30°C. Presence of the cDNA and correct sequence of the clones were confirmed by both endonuclease digestion and sequencing analysis with pNZ8148 fwd and rev primers (Table 2). The recombinant vector was termed pNZ-HTC.

Table 2: Oligonucleotides primers used for cloning and sequencing

Oligonucleotides	Sequence 5'-3'
pKL-NcoIm fwd	GGGCGCGGATCC**ATG***GGA*CATCATCATCATCATC
pKL-NcoIm rev	GATGATGATGATGATG*TCC***CAT**GGATCCGCGCCC
pNZ8148 fwd	CGCGAGCATAATAAACGGCTCTG
pNZ8148 rev	GTGTTGCTTTGATTGATAGCCAAAAAGC

Induction of membrane protein expression

Precultures in M17G1Chl inoculated with frozen stock from both C- (negative control corresponding to bacteria transformed with the empty vector) and HTC recombinant bacteria were incubated overnight at 30°C with gentle shaking (90 rpm). They were added at 1/40 (v:v) to 250mL M17G1Chl in Schott bottles and incubated at 30°C with gentle shaking (90 rpm) until the OD reached 0.75-0.80 (for details, see [31]). At this time, induction was performed by addition of nisin obtained from supernatant of culture of NZ9700 strains [32]. Incubation were

pursued for 4 additional hours, optimal duration of induction suitable for higher level of MP expression in *L. lactis* [27-33]. Bacteria were harvested by centrifugation at 5000 *g* for 15 min at 4°C. The pellets were resuspended, washed in buffer TN (50 mM Tris-HCl, 150 mM NaCl, pH 7.5) and centrifuged at 5000 *g* for 15 min, at 4°C one more time. The bacterial pellets were kept at −80°C after resuspension in TN until isolation.

Isolation of crude bacterial membrane proteins

The bacteria were disrupted by 2-fold passages through a One Shot (Constant Cell Disruption Systems, Northants, UK) at 35,000 p.s.i. (2.3 kbars) and kept on ice until centrifugation. After cell breakage, the lysates were centrifuged at 10,000 *g* for 10 min, at 4°C, and the supernatant containing proteins was transferred into centrifuge tubes for further ultracentrifugation at 150,000 *g* for 1 h, at 4°C. MPs present in pellets were resuspended in TN/1% glycerol and kept at −80°C.

SDS-Polyacrylamide Gel Electrophoresis and Western blotting

Protein content of membrane fractions were estimated using the Bio-Rad protein assay reagent (Bio-Rad, Hercules, CA). Equal quantity of protein of each sample was mixed with 4x sample buffer and heated at 95 °C for 10 min before separation by SDS polyacrylamide gel electrophoresis using a 4-12% gradient gel at the same time as a positive control (15 µg) corresponding to total MPs isolated from Sf21 insect cells transformed with the pKL/HTC plasmid [20] and expressing caveolin-1β at about 3% of total MPs (personal communication). For Western blotting, proteins were transferred to nitrocellulose membranes (10600019, Amersham), and blocked using 5% skim milk. Membranes were incubated either with

antibody against caveolin (1/7000; 610407, BD Science, USA) and then with secondary anti-mouse HRP-conjugated antibodies (1/3000; 170-6516, Bio-Rad, USA) or with His-HRP conjugate (1/5000; 15165, Fisher). Detection was then performed through enhanced chemiluminescence (ECL) with a ChemiDoc system (Bio-Rad, USA). Bands corresponding to the proteins were analyzed and quantified through ImageLab software.

Density gradient ultracentrifugation

First, 1.25 mg of total membrane proteins isolated from both EV and HTC recombinant bacteria cultured and isolated at the same time were loaded on a discontinuous sucrose gradient from 20 to 44%. After ultracentrifugation at 150,000 × *g* for 19 h at 4°C, 24 fractions of 500 µL were then collected. Each fraction was divided into aliquots before storage at −80°C before further analysis. Sucrose density was measured for each fraction using a refractometer (Carl Zeiss, 47729), and appeared to be almost similar for both C- and HTC fractions from 1 to 24; linear regression gave equivalent coefficients and R^2 superior to 0.98.

Dynamic Light Scattering (DLS) analysis

Particle diameters were measured by DLS (NanoZS, Malvern) with a 633 nm laser. Measurements were taken on samples diluted 1:100 (v:v) in PBS1x using cuvette (ZEN0040, Malvern). The viscosity of PBS1x is 0.87 cP and the refractive index is 1.33. The refractive index of the particles was taken to be 1.52. Data were recorded as an average of 13 five-second acquisitions. Measurements were performed in triplicate at 25 °C. Recorded data were analysed in number with the Zetasizer software, which also calculated the polydispersity index

of the samples (ranging from 0 for a perfectly monodisperse homogeneous sample to 1 for a highly polydisperse heterogeneous sample).

Transmission Electron Microscopy (TEM) ultrastructural analysis

L. lactis bacteria were transferred to aluminium sample holders and cryoimmobilized immediately using a Leica High-Pressure Machine (HPM 100, Leica Microsystems, Vienna, Austria), and then transferred to liquid nitrogen. Samples were then freeze substituted in a Leica AFS system (Leica Microsystems, Vienna, Austria) with 1% OsO4 in anhydrous acetone with 1% glutaraldehyde, and 1% water at –90°C for 1 day, followed by slow warming to room temperature over a period of 7 days. After rinsing in several acetone washes, samples were then gradually infiltrated with mixtures of acetone/epoxy resin and pure epoxy resin (EMbed 812 resin kit, Electron Microscopy Sciences, Hatfield, United States) for 31 hours. Samples were embedded in fresh Epon and polymerized at 60°C for 48 h. Ultrathin sections (90 nm) were cut on a Reichert Ultracut E ultramicrotome (Leica, Rueil-Malmaison, France), examined in transmission electron microscope (HITACHI H7800, Japan) operating at 80 kV, and photographed with an AMT nanosprint 43 camera (AMT, Woburn, USA) on the DIMACELL platform (INRAE, Dijon, France).

Immuno-electron microscopy (IEM)

For immunolabeling of high-pressure frozen samples, the freeze substitution medium consisted of anhydrous acetone containing 0.2% uranyl acetate in the AFS unit as described above at –90°C for 4 days, followed by slow warming to -50°C over a period of 2 days. After

rinsing in several acetone washes, samples were infiltrated in Lowicryl® HM20 resin (MonoStep HM20 resin, Electron Microscopy Sciences, Hatfield, United States) at -50°C, polymerized under UV light, and subsequently sectioned. Ultrathin sections (82 nm) were cut as above and were collected onto carbon-collodion-coated 200-mesh grids. A solution of caveolin antibody diluted at 1/75 and of a goat anti-mouse conjugated with 5-nm colloidal gold diluted 1/25 (secondary antibody) were successively applied prior to TEM observations. These observations were carried out using an electron microscope (HITACHI H7800, Japan) as described above.

Negative staining electron microscopy

Five µL of membrane fraction sample was placed on an effluved carbon formvar grid and allowed to rest for 20 min before blotting with filter paper. Samples were negative stained with commercial solution (Uranyless EMS, USA) during 3 min before blotting and air drying. Transmission electron microscopy (TEM) images were taken with a Hitachi H7800 at an acceleration voltage of 100 kV and an AMT camera.

Results

- **Cloning of Caveolin-1β within the pNZ8148 vector**

In the present study, we chose to express the caveolin-1β isoform X1 from *Canis lupus familiaris*. This isoform displays 93.5% of identity with the human gene. The 10His-tag affinity tag has been added to the N-terminus of the gene to help further detection and affinity

purification of the protein, and due to the involvement of the C-terminus for the conformation and functionality of the protein [34].

To generate recombinant *L. lactis* strains, cDNA encoding for the protein of interest was subcloned into pNZ8148 vector. This vector possesses the nisin inducible promoter with the obligatory *Nco*I site for translational fusions [35]. Since the pKL/HTC recombinant vector does not hold the *Nco*I site at the ATG of the gene, a mutagenesis was first performed in *E. coli* to insert this restriction site simultaneously with a codon encoding for glycine between the ATG and the second codon of the gene. After digestion with restriction enzymes and ligation, the clone pNZ8148-HTC was successfully generated (called pNZ-HTC).

- **Caveolin-1β is expressed at high levels in *L. lactis* membranes**

After cloning into pNZ8148, the expression of caveolin-1β has been tested in *L. lactis*. After 4 hours of nisin induction, bacteria were disrupted, and both soluble and membrane proteins were analyzed by Western blot with antibodies specific either to the protein (Fig. 1A) or to the affinity tag used (Fig. 1B).

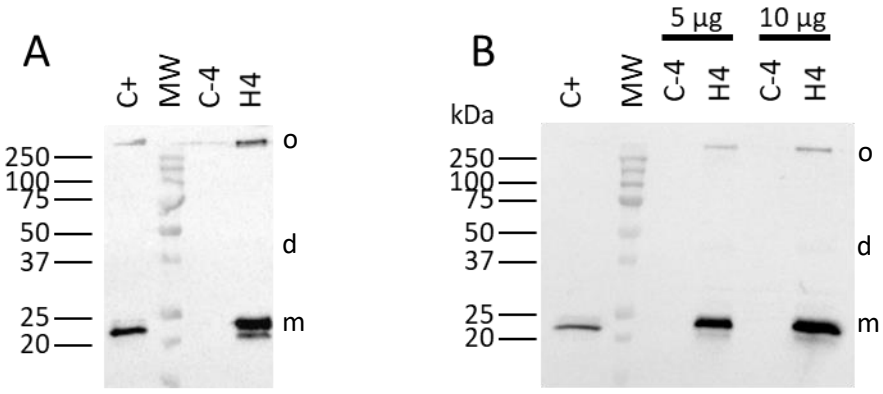

Figure 1: Expression of HTC in L. lactis after 4 hours post-induction by nisin. Total membrane proteins (5 µg for panel A, 5 and 10 µg for panel B) were separated in a 12% SDS-PAGE and analyzed by Western

blot performed using either an antibody specific to caveolin-1 (panel A; 1/7500) or an HRP-conjugate specific to the His-tag affinity tag (panel B; 1/5000). A positive control protein containing caveolin-1β (C+; 15 µg) and the band of 75 kDa of the molecular weight from Bio-Rad (constitutively His-tagged) were used to estimate the expression levels of the recombinant proteins. H means membrane proteins derived from bacteria containing the recombinant pNZ-HTC vector, C- means crude membrane proteins derived from control bacteria containing the empty pNZ8148 vector. o,d,m correspond respectively to oligomer, dimer and monomer. Western blot images are merged images of both colorimetric analysis of membranes revealing the molecular weights and chemiluminescent analysis revealing only some molecular weight bands.

Caveolin-1β was successfully expressed in *L. lactis* and was only present in the membrane fractions. Indeed, Western blot analysis of soluble fractions using the same antibody did not show any band (data not shown). No band was observed in the negative control (C-4) corresponding to the proteins isolated from bacteria transformed by the empty vector. We noticed the presence of additional bands at around 45 and 250 kDa, at the interface between the stacking and concentration parts of the SDS-PAGE, corresponding to the dimer and oligomers of caveolin-1β, respectively. Absence of heating of the samples before the SDS-PAGE led to an increase of the amount of these oligomers from about 10% to about 50% of the total caveolin-1β expression (Fig. S1). Following two independent protein quantification in triplicate using either the intensity of the 75 kDa band from Bio-Rad molecular weight (161-0373) or the positive control from Sf21 cells, the recombinant protein produced has been consistently estimated to represent about 25 % of total MPs (Fig. 1A and 1B), a remarkably high expression level for an eukaryotic MP expressed in *L. lactis*.

Subsequently, different induction times, including shorter and longer times, were tested to check the impact of induction time on protein expression level.

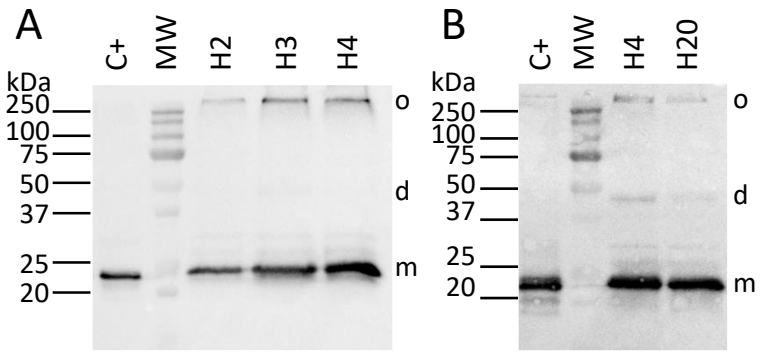

Figure 2: Expression of HTC in L. lactis depending as a function of induction time. A. Impact of short times of induction on protein expression (2-, 3- and 4-hours post-induction). B. Impact of long time of induction on protein expression (4- and 20-hours post-induction). Total membrane proteins (10 µg) were separated in a 12% SDS-PAGE and analyzed by Western blot performed using an HRP conjugate specific to the His-tag affinity tag. A positive control protein containing caveolin-1β (C+; 15 µg) was loaded and the band at 75 kDa of the molecular weight from Biorad was used to estimate the expression levels of the recombinant protein. o,d,m correspond respectively to oligomer, dimer and monomer.

Interestingly and as expected, the amount of protein produced was higher after 4 hours of induction, as depicted on Fig. 2A. This duration has already proved to be optimal for the expression in *L. lactis* of various MPs of diverse origins [27,33]. This time of duration was thus chosen for all the further experiments performed within this study, except for microscopy. The amount of protein expressed after 20 h post-induction was also studied to verify the amount of protein produced prior to microscopic analysis. As depicted on Fig. 2B, this amount was still relatively high, almost similar to those obtained after 4 hours of

induction, and appropriate for further microscopic analysis on bacteria. Moreover, additional bands corresponding to dimer and oligomer were also observed.

In conclusion, the protein caveolin-1β can be heterologenously expressed in *L. lactis*, at high levels and under its oligomeric state.

- **Caveolin-1β is found in membranes of different densities after discontinuous gradient**

Equal quantities of total MPs (1.25 mg) from 3 different experiments were loaded on discontinuous sucrose gradient to separate the membranes collected after cell disruption depending on their density. In Fig. 3 are presented the Western blotting results of the different fractions obtained from one experiment representative of three.

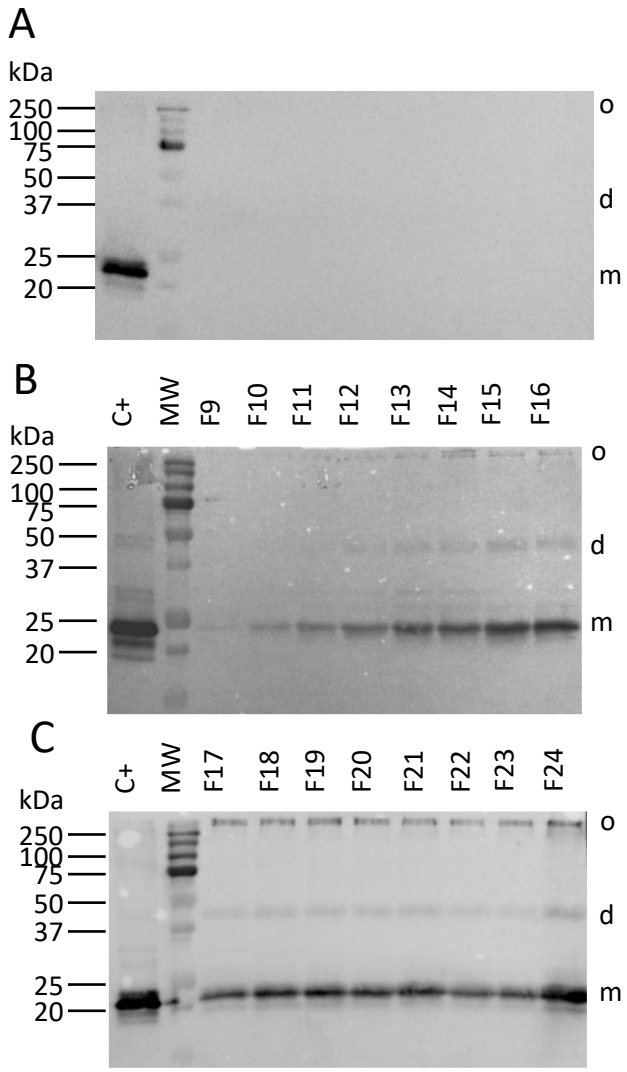

Figure 3: Expression of HTC in fractions after sucrose gradient. A. Expression in fractions from 1 to 8. B. Analysis of fractions from 9 to 16. C. Fractions from 17 to 24. Equal volumes of fractions (20 µL) were separated in a 12% SDS-PAGE and analyzed by Western blot performed using an HRP-conjugate specific to the His-tag affinity tag. A positive control protein sample containing caveolin-1β (C+; 15 µg) was loaded. o,d,m correspond respectively to oligomer, dimer and monomer.

A band at around 20-25 kDa, like that found in the positive control, was found in the fractions from 10 to 24, but absent in the first lighter fractions (from 1 to 8, a weak band in 9). The bands corresponding to the dimer (45 kDa) and the oligomer (250 kDa) started to appear

311 in fraction 12 and in fraction 14 respectively and remained present in all the denser fractions.
312 The intensity of all bands was higher in the final fraction 24 that corresponded to the pellet of
313 the gradient. No band was observed in the fractions isolated from the negative control.

314 The presence, in fractions of different densities, of caveolin-1β in its oligomeric state
315 suggested that the protein could possibly be functional, according to the literature reporting
316 on the necessary caveolin-1 oligomerization for inducing membrane curvature [8,9] (see
317 Discussion section).

318

319 - ***Lactococcus lactis*** **produces caveolin-1β enriched intracellular vesicles**

320 Both caveolin-1β expressing and control bacteria were analyzed through transmission
321 electron microscopy (TEM) 20 hours post-induction to see whether the bacteria were able to
322 produce intracellular vesicles and their subcellular localization. Immunolabelling and cryo-
323 TEM were used to observe the presence of such vesicles and to determine their diameter.

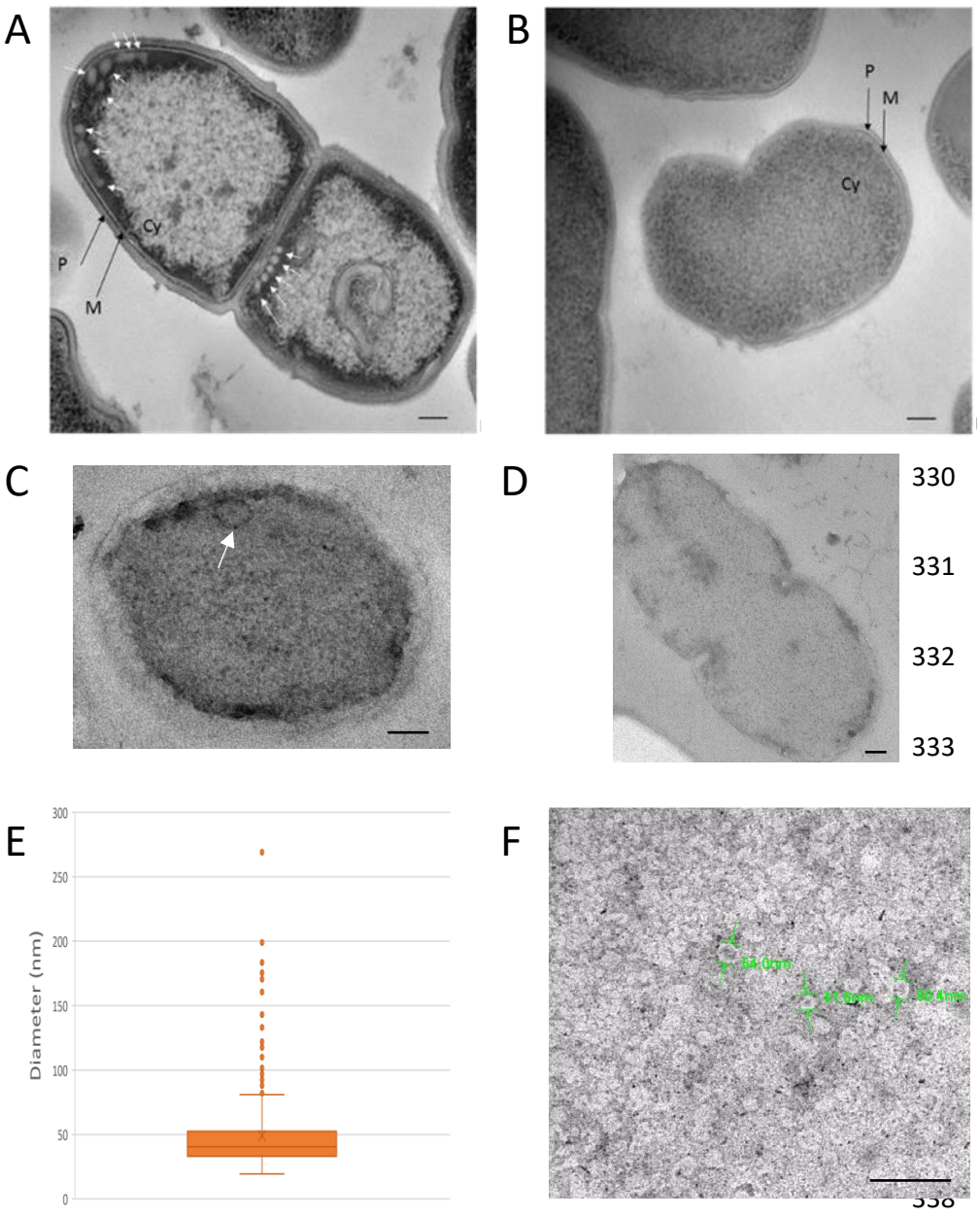

Figure 4: Transmission electron microscopy (TEM) analysis. A and B. Cryo-TEM of recombinant bacteria containing either pNZ-HTC or the empty vector (C-). A. TEM of HTC bacteria displayed the presence of vesicle near the plasma membrane. B. TEM of C- bacteria. Scale=100 nm (A and B). C and D. Immunolabelling of bacteria harboring either HTC (C) or the empty vector (C-; D). Scale=100 nm. E. Distribution of diameters of intracellular caveolin-1β enriched vesicles determined from TEM images (n=390; N=2); the orange region depicts the 75% most frequent values. F. Negative staining-TEM

images from vesicles isolated through density discontinuous gradient fraction F15 (scale=200 nm). P = peptidoglycan, M = plasma membrane, Cy = cytoplasm.

Remarkably, vesicles were present close to the plasma membrane, mostly at the apex of HTC bacteria (Fig. 4A), whereas none was observed in the negative control bacteria (Fig. 4B). Immunolabelling was performed, using the same antibody as that used for Western blot analysis, and revealed the localization of these antibodies within the intracellular vesicles (Fig. 4C), while no immunodetection was observed in the plasma membrane devoid of such internal vesicles (Fig. 4D). All the observed vesicles (n=390) were measured, allowing to determine a mean diameter of 50.3 +/- 18.7 nm (Fig. 4E), and to estimate that almost 75% of vesicles displayed a diameter between 30 to 60 nm, with a median value of 40.2 nm. The number of vesicles contained in all the entirely imaged bacteria was determined to be 351 in 77 whole and entire bacteria, corresponding to a mean number of 4.6 vesicles/cell. However, TEM imaging can only detect vesicles present within the observed slice of 90 nm thickness, cut from a whole bacterium of diameter roughly ten times larger, and this requires a geometric correction for evaluating the number of intracellular vesicles (Fig. S2). Assuming in a first approach a spheric bacteria and an equatorial cylinder of the same diameter for modeling the TEM section, the volume ratio is about 7, meaning that we must consider that there are about 30 vesicles in each *L. lactis* cell overexpressing caveolin-1β. For the sake of comparison with the vesicles isolated from these bacteria after their disruption, negative staining-TEM analysis of the fraction F15, corresponding to 31.25 % sucrose, displayed vesicles with diameters of 52 +/- 8 nm (n=102) (Fig. 4F).

- **Vesicles containing caveolin-1β display different diameters after discontinuous density gradient**

After biochemical analysis, the fractions were analyzed by dynamic light scattering (DLS) to determine the vesicle diameter. The fractions from both types of total MPs (C- and HTC) of three independent experiments were analyzed (Fig. 5).

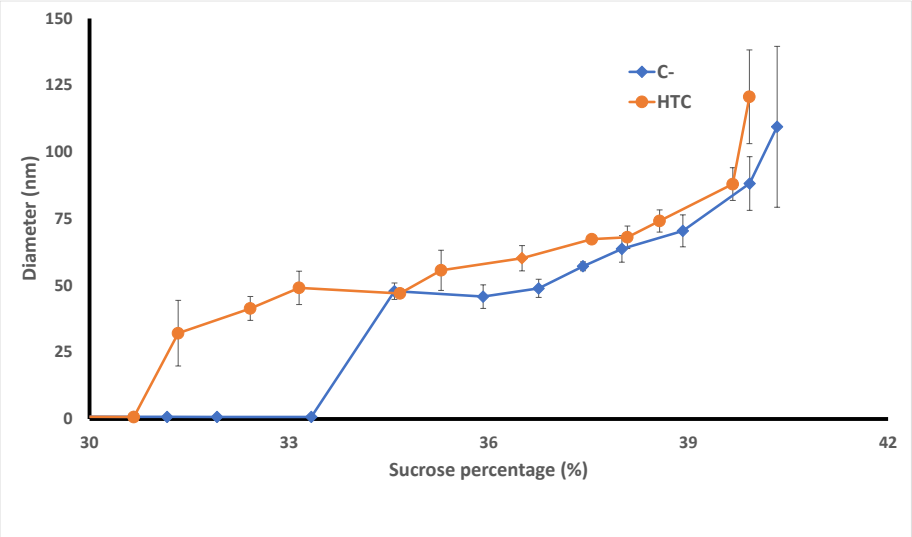

Figure 5: DLS analysis of fractions depending on sucrose percentage in fractions. Fractions were diluted 1/100 in PBS1x pH7.4 prior to analysis. HTC (orange circles) and C- (blue diamonds). N=3; results are mean of 9 different measurements since the NanoZS apparatus perform three determinations per sample.

HTC and C- fractions displayed different size profiles. First, no vesicle was detected and measured in fractions F1-F13 up to 31% of sucrose for both types of fractions, although some amounts of MPs were readily present when assayed in these fractions (data not shown). Then, for the fractions F14-F16 between 31 and 34% sucrose, vesicles from 30 to 50 nm (mean diameter 40.9 +/-8.0 nm) were detected and measured only in the HTC fractions, but not in the C- fractions. Their polydispersity indexes were measured between 0.25 and 0.30, revealing

385 a relatively high homogeneity in size. Then, for increasing densities above 34.5% sucrose,
386 fractions F17-F24 of both HTC and C- bacteria displayed vesicles with increasing diameters,
387 from 50 to about 120 nm. At each density, vesicles from HTC fractions displayed a tendency
388 for a higher diameter than those from C- fractions (almost 7 to 10 nm of difference).

389

390 **Discussion**

391 By comparison with the few eukaryotic and prokaryotic expression systems already
392 tested and reported [16-18,21], the heterologous expression of caveolin-1β in the $Gram^+$
393 bacterial host *L. lactis* has allowed to draw some clues about its relationships within its
394 membrane environment.

395 - *Caveolin-1β is expressed at a remarkably high level for an eukaryotic MP expressed in*
396 *L. lactis*

397 Caveolin-1β expression was tested in *L. lactis* bacteria using the NICE system. After 4
398 hours of nisin induction, bacteria were able to express caveolin-1β at an unexpectedly high
399 expression level for an eukaryotic MP, around 25% of total MPs (Fig. 1A-B), when compared
400 to other eukaryotic MPs previously expressed in the same bacterial host, i.e. typically between
401 1 to 5% of total MPs [30]. Comparison of this relatively high production yield with that
402 obtained for different forms of caveolin within other heterologous expression systems is
403 difficult since quantified data are not available [16-18,21].

404 The relatively high expression of caveolin-1β we obtained could be linked to different
405 features of the protein and/or the host *L. lactis*.

First, it could be related to the caveolin-1β conformation and insertion characteristics within the lipid bilayer. As a matter of fact, only one eukaryotic MP has been expressed in *L. lactis* at a high level comparable to that obtained with caveolin-1β, the plant chloroplastic oxoene reductase ceQORH [33]. This extrinsic protein associates with *L. lactis* plasma membrane by interacting with the membrane polar interface through similar electrostatic interactions as in its native organelle, chloroplast [36]. Other proteins belonging to the same family have been shown to be also dimeric, possibly also the case for the ceQORH in a favorable environment such as *L. lactis* even if it was monomeric in *E. coli* [37]. By analogy, it could be considered that caveolin-1β, which is a small MP inserted only into one leaflet of the membrane by a helix-break-helix motif, would rather easily find a "well-suited" membrane environment in *L. lactis*. Anyway, thanks to its high level of production in a functional, membrane curving state, our data open the way to the determination of caveolin-1β structure using *L. lactis* as a bacterial host.

Second, this relatively high expression level could also be linked to the specific lipid composition of *L. lactis*. Prakash et al (2022) [38] highlighted the importance of cholesterol, phosphatidylserine [21,39], sphingomyelin and glycosphingolipids in caveolin-1 mediated membrane curvature. Yet *L. lactis* does not possess such lipids within its membrane, but in contrast it displays notably large amounts of cardiolipin (42.5 % mol/mol) [40]. This lipid has already been demonstrated to play an important role in MP stability [41], microdomain formation [42] and membrane curvature [43], some properties shared with cholesterol [10]. Hence, cardiolipin could act to stabilize caveolin-1β within the membrane, therefore favoring its expression and functionality to induce intracellular vesicles formation within bacteria. However, it should be noted that caveolin-1β is believed to insert into the external leaflet of the vesicles, due to a wedge effect [44], whereas cardiolipin is expected to segregate within

its internal leaflet of the membrane (due to its small polar headgroup). This means that such stabilizing effect of cardiolipin on caveolin-1β should be considered as indirect, even if potentially relevant for helping it to contribute for generating membrane curvature. Indeed, the intracellular caveolar vesicles were observed by EM to be mainly present at the apex of the cells, in particular at the bacteria division sites (Fig. 4A), a region where the plasma membrane is rather curved and reported in *E. coli* to be enriched in cardiolipin [42,45-46]. The fact that these vesicles were observed at the septum of dividing bacteria is reminiscent of a similar localization for eukaryotic caveolae in non-transfected organisms, where caveolin and caveolae are involved in membrane changes during abscission and cytokinesis [47]. Finally, this situation of MP-lipid relationships is possibly an illustration of the important role of cardiolipin that has been involved for intracellular curved membrane structures formation in *E. coli* when overexpressing some specific MPs [48,49]. Further lipidomic analyses of light and dense vesicles could help to characterize them and to understand the formation of caveolin-1β enriched intracellular vesicles in *L. lactis*.

- *Virtually all expressed oligomerized caveolin-1β is harbored by intracellular neo-formed vesicles*

Electron microscopy (EM) imaging has revealed that the HTC-expressing bacteria presented several intracellular vesicles presenting fairly homogenous size centered around 40-50 nm of diameter (Fig. 4A), while this was not observed in the control cells (Fig. 4B). This illustrates the capacity of caveolin-1β to induce membrane remodeling (directly or not). The location of these vesicles beneath the plasma membrane indicates that they are likely formed from it, or at least from certain sub-domains of the bacterial plasma membrane since they

appeared to be not equally distributed along all the cell membrane. The immuno-labelling experiments further pointed to a clear location of caveolin-1β at the level of these intracellular vesicles, but no labelling of the plasma membrane at distant sites of these vesicles could be detected (Fig. 4C). This shows that caveolin-1β is sufficient, in the absence of any of the protein partners found in mammalian cells exhibiting caveolae, such as cavins, and of bacterial homologues, for being directly responsible for a local membrane curving effect leading to vesiculation with a high efficiency. In addition, EM imaging allowed to grossly evaluate the total quantity of membranes corresponding to the cumulated number of these intracellular vesicles within a transformed bacterium, taking roughly 30 vesicles/cell. Indeed, considering this number and their mean diameter leads to a cumulated area of about 240 000 nm^2 for the total membranes of these intracellular vesicles in each bacterium. The imaged bacteria harbored a total plasma membrane area of about 2 μm^2 for the round "interphasic" ones (c.a. 0.8 µm diameter), while the much more elongated "pre-division" ones (c.a. 0.6 µm width and 1.3 µm length) had an area of about 4 μm^2. These values lead to evaluate that the total amount of membranes of these intracellular vesicles represent about 6 to 12% of the plasma membrane of the transformed HTC bacteria. These neo-formed intracellular vesicles can thus well accommodate the overexpressed oligomerized caveolin-1β, evaluated to be roughly almost the half of the total expressed caveolin-1β and thus about 12-13% (for a total of about 25%). This is thus consistent with the fact that a large majority of the expressed oligomerized caveolin-1β is present in these internal vesicles, which then could be so-called "caveolar vesicles". We propose this term as a proper description for these membrane structures and consider that it is better suited than the previously used appellation "heterologous caveolae" since there is no morphological indication of caveolin-1β expression at the level of the plasma membrane. They are similar in size to the intracellular vesicles produced in *E. coli*, i.e. 45-50

nm diameter [17], but smaller than those produced in insect cells [18], in *Toxoplasma gondii* [21], as well as in the native caveolae [50] that were reported to be 60 to 90 nm of diameter.

- *Caveolar vesicle formation is correlated with caveolin-1β oligomerization*

L. lactis was able to express caveolin-1β in its oligomeric state, since both dimeric and oligomeric forms were observed on the Western blot analyses of both HTC total MPs and membrane fractions (Fig. 1-2-3). Indeed, *L. lactis* can express various MPs under their native oligomeric state [25,27]. The production of such forms underlies the possibility of expression of a functional caveolin-1 able to induce the formation of intracellular vesicles. Only few studies on caveolin-1 expression displayed data on the various forms of the protein and their analyses through Western blots [23,51]. The oligomers are larger than 250 kDa and found at the interface between the two types of SDS-PAGE gels (concentration and separation), even if the samples were heated at 95°C for 10 min in 4% SDS. This phenomenon could be explained by the fact that oligomers are highly resistant to detergents as pointed by Zhang et al. [23] which suggested to boil them prior to SDS-PAGE. Supplementary experiments shown that boiling samples led to a large denaturation of the oligomers (Fig. S1). The fact that some oligomers were still present after boiling could be due to the relatively high amount of caveolin-1β produced in *L. lactis*.

Interestingly, we observed thanks to membrane fractionation that the caveolin-1β oligomers could be detected from the fraction F14 and in all the denser ones (Fig. 3), which is in perfect correlation with the appearance of membrane vesicles from HTC-expressing bacteria as detected by DLS (Fig. 5). This observation thus provides strong indication for the requirement of caveolin-1β oligomerization for the intracellular caveolar vesicles formation.

By inference, caveolin-1β monomers (and dimers) should be present in limited amounts in the plasma membrane, where they hence can be hardly immuno-detected.

- *The formed caveolar vesicles display a certain heterogeneity in density*

Data obtained by Western blotting and DLS analysis of membrane fractions have been combined to analyze the nature of vesicles isolated and to distinguish the different types of populations observed by DLS analysis. For the control bacterial cells, DLS measurements have shown that the lighter membrane fractions F1 to F16 did not display any detectable vesicles, although they contain nearly the half of the MPs (data not shown). This shows that a notable part of the disrupted plasma membrane produced non-vesiculated membrane fragments of low density, and only the denser fractions (F17 to F24) were able to form revesiculated membranes after the cell disruption. In the membrane fractions obtained from HTC-expressing bacteria, the light ones F10-F13 contained caveolin-1β monomers (and some dimers) but no vesicle structures, while DLS could detect membrane vesicles in the fractions F14-F16. This means that these light vesicles, containing caveolin-1β (with some oligomers, as stated above) are formed before bacterial cell disruption, and are attributable to the lightest part of the intracellular caveolar vesicles. In the denser fractions F16 to F24, there is thus a coexistence of denser caveolar vesicles and revesiculated plasma membrane fragments.

Thus, density sucrose fractionation allowed separating two types of vesicles containing caveolin-1β out of the total MPs, i.e. small and light vesicles of 30 to 50 nm of diameter and larger vesicles from 50 to 120 nm in denser fractions. The light caveolar vesicle fraction F15 has been observed by EM, and this allowed to measure their mean size, which was found in good agreement with the DLS data. These light caveolar vesicles being most probably characterized by a lower protein-to-lipid ratio than the denser ones, this means they should

523 contain only few endogenous MPs, if any, (which otherwise cannot revesiculate after cell
524 disruption) besides caveolin-1β oligomers, considering that caveolin oligomers are reported
525 to exert their membrane curving effect according to rather defined stoichiometric ratios
526 [1,8,45]. In contrast, the denser caveolar vesicles, hence with a higher protein-to-lipid ratio
527 and presenting a somehow constant number of oligomers immuno-detected in fractions F17
528 to F24 (Fig. 3C), should contain some higher amounts of endogenous MPs. This progressive
529 change in MP composition, from F17 to F24, happened to be correlated with a significant
530 increase of the vesicle size as measured by DLS (Fig. 5), even if this technique cannot *per se*
531 separate the respective contributions of the two vesicle populations coexisting in these
532 density fractions. Of note, our study is one of the rare one determining caveolar vesicle
533 diameter through DLS, since most reports of vesicle diameter determinations were performed
534 through TEM analyses. This technique allows diameter measurements in solution, less
535 perturbing for biological samples including vesicles. The present study followed the "MISEV
536 guidelines" for vesicle analysis since two complementary techniques (DLS and cryo-TEM) have
537 been used for the analysis and gave comparable results [52]. Moreover, polydispersity indexes
538 of vesicles obtained through DLS analysis were relatively low (around 0.3), while working with
539 biological samples, which highlights the "high quality" in term of size of vesicles produced by
540 *L. lactis*. However, DLS only allows measurement of mean vesicle diameters but does not
541 provide information on the concentration of these vesicles in each fraction, especially in case
542 of size heterogeneity. If available, this additional information would provide insights on the
543 mode of production of these vesicles within the bacteria, and in particular allowing to estimate
544 the proportion of light and dense caveolar vesicles without the need to biochemically separate
545 them. Currently, almost none of the techniques of determining vesicle concentration can

546 reliably measure vesicles smaller than 50 nm in diameter in solution [53]. Future analyses by
547 different techniques, alone or in combination, are needed to refine these aspects.

548 The production by *L. lactis* of internal dense caveolar vesicles containing various
549 endogenous MP normally resident in the plasma membrane (preliminary proteomic data not
550 shown) provides the indication that caveolin-1β biosynthesis occurs, at the level of the plasma
551 membrane, in domains that are shared with the biosynthesis of at least some of the MPs of
552 the bacterial host. Such functional domains appear thus similar to the so-called transertion
553 domains described for *E. coli* and *Bacillus subtilis*, that allow concerted transcription,
554 translation and membrane insertion of neo-synthesized MPs [54]. These membrane domains
555 have been recognized to play a pivotal role for the appearance of various ectopic intracellular
556 membrane structures induced by overexpression of some MPs in bacteria [49]. Indeed, these
557 domains allow the recruitment in the close membrane vicinity of the neo-synthesized
558 caveolin-1β of various MPs before vesiculation occurs. Consequently, this will lead to the
559 formation of a new intracellular membrane compartment harboring some endogenous
560 plasma membrane MPs, the nature of which depending on their affinity with the locally
561 selected lipids and on their ability to accommodate within a curved membrane. In a
562 prospective frame, this opens the interesting possibility that heterologous co-expression of
563 caveolin-1β with another MP (whatever its biological origin) could lead this MP to be similarly
564 handled within these neo-formed intracellular caveolar vesicles.

565

566 **Conclusion**

567 Interestingly, *L. lactis* has been shown not only to express caveolin-1β at an unexpectedly high
568 expression level for an eukaryotic MP, but also under its functional oligomeric form, allowing

569 the formation of intracellular vesicles from 30 to 60 nm. Since *L. lactis* does not possess the
570 protein partners and the lipids known to be necessary for caveolae formation, further
571 investigations involving proteomic and lipidomic analyses would allow to decipher the
572 molecular mechanisms involved in the formation of these neo-formed intracellular vesicles in
573 *L. lactis*. Moreover, such heterologous nanovesicles could provide biological materials well-
574 suited for improving MPs functional and structural characterization, as well as they could be
575 used for various biotechnological purposes, including delivery of therapeutics.

576

577 **Bibliography**

578 1- Parton RG, McMahon KA, Wu Y. Caveolae: Formation, dynamics, and function. Curr Opin
579 Cell Biol. 2020a Aug;65:8-16. doi: 10.1016/j.ceb.2020.02.001.

580 2- Jia G, Sowers JR. Caveolin-1 in Cardiovascular Disease: A Double-Edged Sword. Diabetes.
581 2015 Nov;64(11):3645-7. doi: 10.2337/dbi15-0005.

582 3- Campos A, Burgos-Ravanal R, González MF, Huilcaman R, Lobos González L, Quest AFG. Cell
583 Intrinsic and Extrinsic Mechanisms of Caveolin-1-Enhanced Metastasis. Biomolecules. 2019 Jul
584 29;9(8):314. doi: 10.3390/biom9080314.

585 4- Dudău M, Codrici E, Tanase C, Gherghiceanu M, Enciu AM, Hinescu ME. Caveolae as
586 Potential Hijackable Gates in Cell Communication. Front Cell Dev Biol. 2020 Oct 27;8:581732.
587 doi: 10.3389/fcell.2020.581732.

588 5- Simón L, Campos A, Leyton L, Quest AFG. Caveolin-1 function at the plasma membrane and
589 in intracellular compartments in cancer. Cancer Metastasis Rev. 2020 Jun;39(2):435-453. doi:
590 10.1007/s10555-020-09890-x.

6- Low JY, Laiho M. Caveolae-Associated Molecules, Tumor Stroma, and Cancer Drug Resistance: Current Findings and Future Perspectives. Cancers (Basel). 2022 Jan 25;14(3):589. doi: 10.3390/cancers14030589.

7- Kirkham M, Nixon SJ, Howes MT, Abi-Rached L, Wakeham DE, Hanzal-Bayer M, Ferguson C, Hill MM, Fernandez-Rojo M, Brown DA, Hancock JF, Brodsky FM, Parton RG. Evolutionary analysis and molecular dissection of caveola biogenesis. J Cell Sci. 2008 Jun 15;121(Pt 12):2075-86. doi: 10.1242/jcs.024588.

8- Hayer A, Stoeber M, Bissig C, Helenius A. Biogenesis of caveolae: stepwise assembly of large caveolin and cavin complexes. Traffic. 2010 Mar;11(3):361-82. doi: 10.1111/j.1600-0854.2009.01023.x.

9- Parton RG, del Pozo MA. Caveolae as plasma membrane sensors, protectors and organizers. Nat Rev Mol Cell Biol. 2013 Feb;14(2):98-112. doi: 10.1038/nrm3512.

10- Jarsch IK, Daste F, Gallop JL. Membrane curvature in cell biology: An integration of molecular mechanisms. J Cell Biol. 2016 Aug 15;214(4):375-87. doi: 10.1083/jcb.201604003.

11- Scheiffele P, Verkade P, Fra AM, Virta H, Simons K, Ikonen E. Caveolin-1 and -2 in the exocytic pathway of MDCK cells. J Cell Biol. 1998 Feb 23;140(4):795-806. doi: 10.1083/jcb.140.4.795.

12- Parton RG, Simons K. The multiple faces of caveolae. Nat Rev Mol Cell Biol. 2007 Mar;8(3):185-94. doi: 10.1038/nrm2122.

13- Parton RG, Hanzal-Bayer M, Hancock JF. Biogenesis of caveolae: a structural model for caveolin-induced domain formation. J Cell Sci. 2006 Mar 1;119(Pt 5):787-96. doi: 10.1242/jcs.02853.

613 14- Zhou Y, Ariotti N, Rae J, Liang H, Tillu V, Tee S, Bastiani M, Bademosi AT, Collins BM,
614 Meunier FA, Hancock JF, Parton RG. Caveolin-1 and cavin1 act synergistically to generate a
615 unique lipid environment in caveolae. J Cell Biol. 2021 Mar 1;220(3):e202005138. doi:
616 10.1083/jcb.202005138.

617 15- Porta JC, Han B, Gulsevin A, Chung JM, Peskova Y, Connolly S, Mchaourab HS, Meiler J,
618 Karakas E, Kenworthy AK, Ohi MD. Molecular architecture of the human caveolin-1 complex.
619 Sci Adv. 2022 May 13;8(19):eabn7232. doi: 10.1126/sciadv.abn7232.

620 16- Li S, Song KS, Lisanti MP. Expression and characterization of recombinant caveolin.
621 Purification by polyhistidine tagging and cholesterol-dependent incorporation into defined
622 lipid membranes. J Biol Chem. 1996 Jan 5;271(1):568-73. PMID: 8550621.

623 17- Walser PJ, Ariotti N, Howes M, Ferguson C, Webb R, Schwudke D, Leneva N, Cho KJ, Cooper
624 L, Rae J, Floetenmeyer M, Oorschot VM, Skoglund U, Simons K, Hancock JF, Parton RG.
625 Constitutive formation of caveolae in a bacterium. Cell. 2012 Aug 17;150(4):752-63. doi:
626 10.1016/j.cell.2012.06.042.

627 18- Li S, Song KS, Koh SS, Kikuchi A, Lisanti MP. Baculovirus-based expression of mammalian
628 caveolin in Sf21 insect cells. A model system for the biochemical and morphological study of
629 caveolae biogenesis. J Biol Chem. 1996 Nov 8;271(45):28647-54. doi:
630 10.1074/jbc.271.45.28647.

631 19- Li S, Galbiati F, Volonte D, Sargiacomo M, Engelman JA, Das K, Scherer PE, Lisanti MP.
632 Mutational analysis of caveolin-induced vesicle formation. Expression of caveolin-1 recruits
633 caveolin-2 to caveolae membranes. FEBS Lett. 1998 Aug 28;434(1-2):127-34. doi:
634 10.1016/s0014-5793(98)00945-4.

635 20- Perrot N, Dessaux D, Rignani A, Gillet C, Orlowski S, Jamin N, Garrigos M, Jaxel C. Caveolin-
636 1β promotes the production of active human microsomal glutathione S-transferase in induced
637 intracellular vesicles in Spodoptera frugiperda 21 insect cells. Biochim Biophys Acta
638 Biomembr. 2022 Aug 1;1864(8):183922. doi: 10.1016/j.bbamem.2022.183922.

639 21- Lige B, Romano JD, Sampels V, Sonda S, Joiner KA, Coppens I. Introduction of caveolae
640 structural proteins into the protozoan Toxoplasma results in the formation of heterologous
641 caveolae but not caveolar endocytosis. PLoS One. 2012;7(12):e51773. doi:
642 10.1371/journal.pone.0051773.

643 22- Jung W, Sierecki E, Bastiani M, O'Carroll A, Alexandrov K, Rae J, Johnston W, Hunter DJB,
644 Ferguson C, Gambin Y, Ariotti N, Parton RG. Cell-free formation and interactome analysis of
645 caveolae. J Cell Biol. 2018 Jun 4;217(6):2141-2165. doi: 10.1083/jcb.201707004.

646 23- Zhang Y, Zhang X, Kong W, Wang S. Reconstitution of Caveolin-1 into Artificial Lipid
647 Membrane: Characterization by Transmission Electron Microscopy and Solid-State Nuclear
648 Magnetic Resonance. Molecules. 2021 Oct 14;26(20):6201. doi: 10.3390/molecules26206201.

649 24- Shin J, Jung YH, Cho DH, Park M, Lee KE, Yang Y, Jeong C, Sung BH, Sohn JH, Park JB, Kweon
650 DH. Display of membrane proteins on the heterologous caveolae carved by caveolin-1 in the
651 Escherichia coli cytoplasm. Enzyme Microb Technol. 2015 Nov;79-80:55-62. doi:
652 10.1016/j.enzmictec.2015.06.018.

653 25- Kunji ER, Slotboom DJ, Poolman B. Lactococcus lactis as host for overproduction of
654 functional membrane proteins. Biochim Biophys Acta. 2003 Feb 17;1610(1):97-108. doi:
655 10.1016/s0005-2736(02)00712-5.

656 26- Kunji ER, Chan KW, Slotboom DJ, Floyd S, O'Connor R, Monné M. Eukaryotic membrane
657 protein overproduction in Lactococcus lactis. Curr Opin Biotechnol. 2005 Oct;16(5):546-51.
658 doi: 10.1016/j.copbio.2005.08.006.

659 27- Bernaudat F, Frelet-Barrand A, Pochon N, Dementin S, Hivin P, Boutigny S, Rioux JB, Salvi
660 D, Seigneurin-Berny D, Richaud P, Joyard J, Pignol D, Sabaty M, Desnos T, Pebay-Peyroula E,
661 Darrouzet E, Vernet T, Rolland N. Heterologous expression of membrane proteins: choosing
662 the appropriate host. PLoS One. 2011;6(12):e29191. doi: 10.1371/journal.pone.0029191.

663 28- Bakari S, André F, Seigneurin-Berny D, Delaforge M, Rolland N, Frelet-Barrand A.
664 Lactococcus lactis, recent developments in functional expression of membrane proteins.
665 2014. Chapter 5 of “Membrane Proteins Production for Structural Analysis”, edited by I.
666 Mus−Vuteau (Springer eBook) pp 107−132.

667 29- Frelet-Barrand A. Lactococcus lactis, an Attractive Cell Factory for the Expression of
668 Functional Membrane Proteins. Biomolecules. 2022 Jan 22;12(2):180. doi:
669 10.3390/biom12020180.

670 30- Mierau I, Kleerebezem M. 10 years of the nisin-controlled gene expression system (NICE)
671 in Lactococcus lactis. Appl Microbiol Biotechnol. 2005 Oct;68(6):705-17. doi: 10.1007/s00253-
672 005-0107-6.

673 31- Frelet-Barrand A, Boutigny S, Kunji ER, Rolland N. Membrane protein expression in
674 Lactococcus lactis. Methods Mol Biol. 2010a;601:67-85. doi: 10.1007/978-1-60761-344-2_5.

675 32- de Ruyter PG, Kuipers OP, de Vos WM. Controlled gene expression systems for Lactococcus
676 lactis with the food-grade inducer nisin. Appl Environ Microbiol. 1996 Oct;62(10):3662-7. doi:
677 10.1128/aem.62.10.3662-3667.1996.

678 33- Frelet-Barrand A, Boutigny S, Moyet L, Deniaud A, Seigneurin-Berny D, Salvi D, Bernaudat
679 F, Richaud P, Pebay-Peyroula E, Joyard J, Rolland N. Lactococcus lactis, an alternative system
680 for functional expression of peripheral and intrinsic Arabidopsis membrane proteins. PLoS
681 One. 2010b Jan 20;5(1):e8746. doi: 10.1371/journal.pone.0008746.

682 34- Plucinsky SM, Glover KJ. Secondary Structure Analysis of a Functional Construct of
683 Caveolin-1 Reveals a Long C-Terminal Helix. Biophys J. 2015 Oct 20;109(8):1686-8. doi:
684 10.1016/j.bpj.2015.08.030.

685 35- Zhou XX, Li WF, Ma GX, Pan YJ. The nisin-controlled gene expression system: construction,
686 application and improvements. Biotechnol Adv. 2006 May-Jun;24(3):285-95. doi:
687 10.1016/j.biotechadv.2005.11.001.

688 36- Miras S, Salvi D, Ferro M, Grunwald D, Garin J, Joyard J, Rolland N. Non-canonical transit
689 peptide for import into the chloroplast. J Biol Chem. 2002 Dec 6;277(49):47770-8. doi:
690 10.1074/jbc.M207477200.

691 37- Mas Y Mas S, Curien G, Giustini C, Rolland N, Ferrer JL, Cobessi D. Crystal Structure of the
692 Chloroplastic Oxoene Reductase ceQORH from Arabidopsis thaliana. Front Plant Sci. 2017 Mar
693 9;8:329. doi: 10.3389/fpls.2017.00329.

694 38- Prakash S, Malshikare H, Sengupta D. Molecular Mechanisms Underlying Caveolin-1
695 Mediated Membrane Curvature. J Membr Biol. 2022 Jun;255(2-3):225-236. doi:
696 10.1007/s00232-022-00236-y.

697 39- Hirama T, Das R, Yang Y, Ferguson C, Won A, Yip CM, Kay JG, Grinstein S, Parton RG, Fairn
698 GD. Phosphatidylserine dictates the assembly and dynamics of caveolae in the plasma
699 membrane. J Biol Chem. 2017 Aug 25;292(34):14292-14307. doi: 10.1074/jbc.M117.791400.

700 40- Oliveira AP, Nielsen J, Förster J. Modeling Lactococcus lactis using a genome-scale flux
701 model. BMC Microbiol. 2005 Jun 27;5:39. doi: 10.1186/1471-2180-5-39.

702 41- Musatov A, Sedlák E. Role of cardiolipin in stability of integral membrane proteins.
703 Biochimie. 2017 Nov;142:102-111. doi: 10.1016/j.biochi.2017.08.013.

704 42- Mileykovskaya E, Dowhan W. Cardiolipin membrane domains in prokaryotes and
705 eukaryotes. Biochim Biophys Acta. 2009 Oct;1788(10):2084-91. doi:
706 10.1016/j.bbamem.2009.04.003.

707 43- Boyd KJ, Alder NN, May ER. Buckling Under Pressure: Curvature-Based Lipid Segregation
708 and Stability Modulation in Cardiolipin-Containing Bilayers. Langmuir. 2017 Jul
709 11;33(27):6937-6946. doi: 10.1021/acs.langmuir.7b01185.

710 44- Parton RG, Kozlov MM, Ariotti N. Caveolae and lipid sorting: Shaping the cellular response
711 to stress. J Cell Biol. 2020b Apr 6;219(4):e201905071. doi: 10.1083/jcb.201905071.

712 45- Mileykovskaya E, Dowhan W. Visualization of phospholipid domains in Escherichia coli by
713 using the cardiolipin-specific fluorescent dye 10-N-nonyl acridine orange. J Bacteriol. 2000
714 Feb;182(4):1172-5. doi: 10.1128/JB.182.4.1172-1175.2000.

715 46- Renner LD, Weibel DB. Cardiolipin microdomains localize to negatively curved regions of
716 Escherichia coli membranes. Proc Natl Acad Sci U S A. 2011 Apr 12;108(15):6264-9. doi:
717 10.1073/pnas.1015757108.

718 47- Andrade V, Bai J, Gupta-Rossi N, Jimenez AJ, Delevoye C, Lamaze C, Echard A. Caveolae
719 promote successful abscission by controlling intercellular bridge tension during cytokinesis.
720 Sci Adv. 2022 Apr 15;8(15):eabm5095. doi: 10.1126/sciadv.abm5095.

721 48- Jamin N, Garrigos M, Jaxel C, Frelet-Barrand A, Orlowski S. Ectopic Neo-Formed
722 Intracellular Membranes in Escherichia coli: A Response to Membrane Protein-Induced Stress
723 Involving Membrane Curvature and Domains. Biomolecules. 2018 Sep 4;8(3):88. doi:
724 10.3390/biom8030088.

725 49- Royes J, Biou V, Dautin N, Tribet C, Miroux B. Inducible intracellular membranes: molecular
726 aspects and emerging applications. Microb Cell Fact. 2020 Sep 4;19(1):176. doi:
727 10.1186/s12934-020-01433-x.

728 50- Bastiani M, Parton RG. Caveolae at a glance. J Cell Sci. 2010 Nov 15;123(Pt 22):3831-6. doi:
729 10.1242/jcs.070102.

730 51- Han B, Tiwari A, Kenworthy AK. Tagging strategies strongly affect the fate of overexpressed
731 caveolin-1. Traffic. 2015 Apr;16(4):417-38. doi: 10.1111/tra.12254.

732 52- Théry C et al. Minimal information for studies of extracellular vesicles 2018 (MISEV2018):
733 a position statement of the International Society for Extracellular Vesicles and update of the
734 MISEV2014 guidelines. J Extracell Vesicles. 2018 Nov 23;7(1):1535750. doi:
735 10.1080/20013078.2018.1535750.

736 53- Serrano-Pertierra E, Oliveira-Rodríguez M, Matos M, Gutiérrez G, Moyano A, Salvador M,
737 Rivas M, Blanco-López MC. Extracellular Vesicles: Current Analytical Techniques for Detection
738 and Quantification. Biomolecules. 2020 May 28;10(6):824. doi: 10.3390/biom10060824.

739 54- Matsumoto K, Hara H, Fishov I, Mileykovskaya E, Norris V. The membrane: transertion as
740 an organizing principle in membrane heterogeneity. Front Microbiol. 2015 Jun 12;6:572. doi:
741 10.3389/fmicb.2015.00572.

742

Acknowledgements

We are grateful to Nadège Jamin and Christine Jaxel (I2BC, Gif-sur-Yvette, France) for her gift of the pKL/HTC plasmid and the caveolin-1β positive control samples. We thank the UMR 1098 – Team TIM-C (Besançon, France) for molecular biology experiments, UMR6213 for access to the NanoZS apparatus; UBFC EA3181 (Besançon, France), INSERM 1231 (Dijon, France) for ultracentrifuge and UMR5086 (Lyon, France), UMR7099 (Paris, France) and UMR PAM (Dijon, France) for access to Cell Disruption system.

Funding

This project was financed by the ANR CAVEOTANK (2017-2021; ANR-17-CE11-0015) and in particular, AF, TB and CL were financed by this source.

Author contribution

AFB conceived the study and secured funding. AFB, AF, PB, ES, SO, AR designed the experiments and analyzed the results. AF, PB, ES, JP, DL, CL, TB performed the experiments. All authors interpreted the data. AFB, AF, PB, ES, DL, SO wrote the initial manuscript and prepared figures. All the authors revised the final manuscript. All authors read and approved the final manuscript.

764